J Nanostruct 16(1): 411-420, Winter 2026

RESEARCH PAPER

Synthesis and Study of the Properties of Some Metal oxide Using Co-Precipitation Method

Safaa A. Yaseen *, We'am Sami

Department of Physics, College of Education, University of Al-Qadisiyah, Qadisiyah, Iraq

ARTICLE INFO

Article History:
Received 19 September 2025
Accepted 02 December 2025
Published 01 January 2026

Keywords:
Calcination
CdO NP
Co-precipitation method
MnONP
Doping of nano-metal oxide

ABSTRACT

In the present work, Cadimum oxide (Cd_xO), Manganese oxide (Mn_xO) and Manganese cadmium oxide ($Mn_xCd_{1-x}O$) nanopowders (where x = 0, 0.5, and 1) were synthesized by a simple chemical co-precipitation method followed with calcination. Physical properties that reported through XRD analysis, FTIR analysis, surface morphology, and Energy dipersive X-ray spectroscopy (EDS). XRD spectra predicted the average size of synthesized Cd_xO nanoparticles is decreased with calcination at 700Ċ for 3 hrs while it was increased for Mn_xO and $Mn_xCd_{1-x}O$ The lattice constant was decreased with increasing of the crystallite size except with Cd_xO**.** The FTIR spectral analysis present reduction in the water-related peaks after calcination indicated successful removal of residual hydroxides and moisture hat help in control particle growth and lead to increase agglomeration. This result shown in FESEM micrographs revealed that the calcination process lead to increase agglomeration. The elemental composition of the nanoparticles was determined by EDS analysis.

How to cite this article
Yaseen S, Sami W. Synthesis and Study of the Properties of Some Metal oxide Using Co-Precipitation method. J Nanostruct, 2026; 16(1):411-420. DOI: 10.22052/JNS.2026.01.037

INTRODUCTION

Metal oxide nanoparticles have attracted significant attention due to their unique chemical, optical, and electronic properties, which differ considerably from their bulk counterparts. Among these, CdO and MnO nanoparticles are widely studied for applications in gas sensing, catalysis, batteries, and optoelectronic devices [1]. Various synthesis routes exist for preparing metal oxide nanoparticles, including sol-gel, hydrothermal, and microemulsion methods.

However, the co-precipitation technique offers notable advantages: simplicity and ease of scaling up [2]. In co-precipitation, metal salts (e.g., chlorides, nitrates) are dissolved in a suitable solvent, and a precipitating agent (often a base) is gradually introduced to form insoluble metal hydroxides. Subsequent drying and calcination transform these hydroxides into the desired oxide phases [3]. By optimizing synthesis parameters—such as pH, temperature, and calcination conditions—researchers can control particle size, crystallinity, and morphology [4].

The large surface area and active sites of metal oxide nanoparticles make them promising for organic transformations and pollution control [5]. Sensors: MnO nanoparticles, in particular, are often employed in gas sensing due to their sensitivity to changes in the ambient atmosphere [6].

Many of the most appealing inorganic minerals is manganese dioxide (MnO_2). Manganese dioxide

* *Corresponding Author Email: safaaameer02@gmail.com*

is a transition metal oxide of P-type semiconductors with a band gap of 3.3 eV and 3.8 eV [7].

Energy Storage that depend on CdO is also studied for its potential in battery electrodes and supercapacitors, owing to its high theoretical capacity [8]. CdO in Optoelectronics has interesting optical properties and is explored in transparent conducting oxide (TCO) applications [1].

Similarly, due to its n-type metallic oxide feature, cadmium oxide (CdO) has been discovered to be useful in Photocatalytic application such as solar cells, photovoltaics, flat displays, and sensors with explicit and implicit band gaps of 2.3 eV and 1.36 eV respectively [9].

Among synthesize routes, co-precipitation method is popularly adopted to synthesize nano-NPs due to its low cost, uniform and high yield of nanoparticles [10].

This paper focuses on synthesizing CdO and MnO nanoparticles using co-precipitation. The prepared samples are characterized by XRD, FTIR, and FESEM to determine phase purity, average crystallite size, functional groups, and surface morphology. Also, EDS test was done to discover the percent of each components of nano oxides after calcination.

MATERIALS AND METHODS

The Fig. 1 shows the steps followed in this study.

Synthesis metal oxide nanoparticles

Preparation methods

Cadimum and Manganese chloride [S.D. Fine. CHEM LTD, 98.0 %] were used as a raw metal source to prepare Cd_xO, Mn_xO and $Cd_xMn_{1-x}O$ nanoparticles where [x= 0, 0.5 and 1].

The co-precipitation method was adopted, which is considered one of the important methods for preparing nanoparticles of similar size due to its high efficiency as well as being an easy and cheap method. This method starts from the core (bottom up) through homogeneous co-precipitation.The co-precipitation method has the following properties:

1. The precipitated material is partially dissolved.
2. Due to supersaturation, a large number of small particles are formed.
3. The saturation state affects the particle size, surface area and the distribution ratios of its particles.
4. The general equation for the co-precipitation method is:

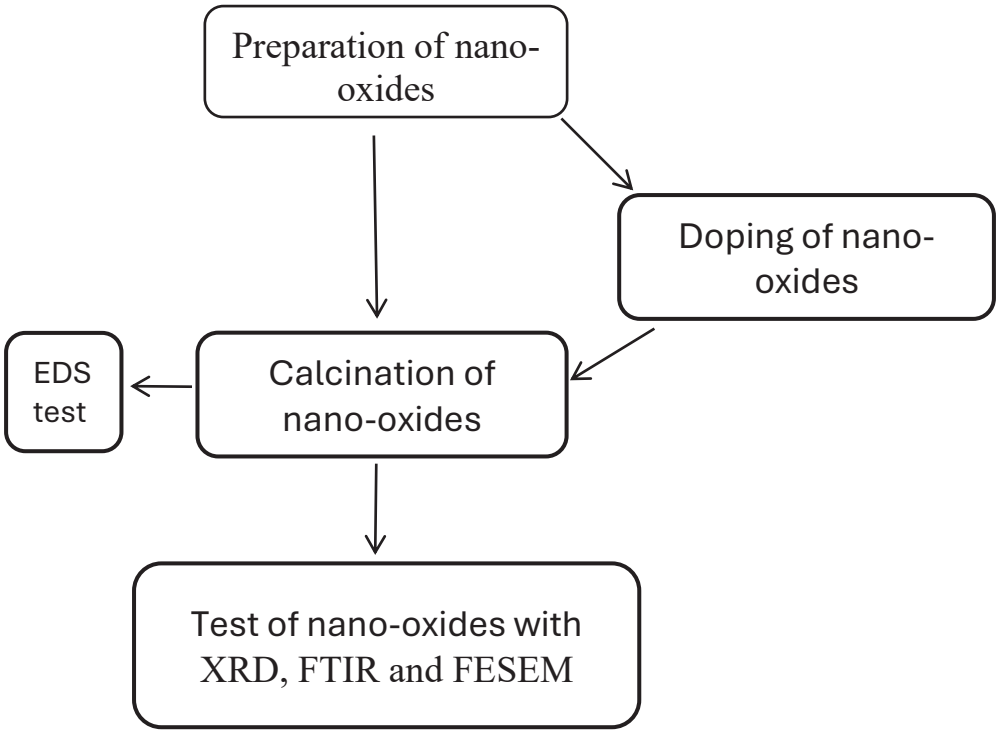

Fig. 1. Block diagram of the study.

$xA^{y+}_{(aq)} + yB^{x-}_{(aq)} \rightarrow AxBy_{(s)}$

5. The co-precipitation reaction can be carried out in different ways such as chemical reduction, oxidation and hydrolysis. Co-precipitation can be carried out by changing some other factors related to solubility such as temperature and concentration [10].

Preparation of Cadimum oxide nanoparticles

0.94 M of aqueous Cadimum chloride $CdCl_2.H_2O$ was prepared by dissolving 11 g of it in 100 ml of deionized water and placing the solution on a magnetic stirrer for 30 minutes until the substance was completely dissolved.

37 ml of sodium hydroxide NaOH [HiMedia, 99.0 %] with a concentration of 3.57 M was added dropwise to bring the pH to 10. Then the precipitate was filtered and washed using deionized water. The precipitate was placed in oven and dried for 6 hours at 100 C. Then it was grind to change the precipitate into powder. After that, the precipitate was placed on Porcelain crucible in furn and burned at 450 C for 3 hours.

$CdCl_2.H_2O + H_2O + 2NaOH \rightarrow CdO + 3H_2O + 2NaCl$

Preparation of Manganese oxide nanoparticles

0.94 M of aqueous nickel chloride $MnCl_2.4H_2O$ was prepared by dissolving 19.5g of it in 100 ml of deionized water and placing the solution on a magnetic stirrer for 30 minutes until the substance was completely dissolved.

44 ml of sodium hydroxide NaOH with a concentration of 3.57 M was added dropwise to bring the pH to 12. Then the precipitate was filtered and washed using deionized water. The precipitate was placed in oven and dried for 6 hours at 100 C. Then it was ground to change the precipitate into powder. After that, the precipitate was placed on Porcelain crucible in furn and burned at 450 C for 3 hours.

$MnCl_2.4H_2O + H_2O + 2NaOH \rightarrow MnO + 6H_2O + 2NaCl$

Doping of Manganese oxide with Cadimum oxide

This doping was carried out by the following procedure:

1. Take 9.75g from MnO mix with 5.5g from CdO

2. Dissolving the mixture in 100ml of deionized water.

3. Placing the solution on a magnetic stirrer for 30 minutes with 30C

temperature until the substance was completely dissolved.

4. 40 ml of sodium hydroxide NaOH with a concentration of 3.57 M

was added dropwise to bring the pH to 9

5. Then the precipitate was filtered and washed using deionized water.

The precipitate was placed in oven and dried for 6 at 100 C. Then it was grind to change the precipitate into powder. After that, the precipitate was placed on Porcelain crucible in furn and burned at 450 C for 3 hours.

$MnCl_2.4H_2O + CdCl_2.H_2O + 4NaOH \rightarrow Mn(OH)_2\downarrow + Cd(OH)_2\downarrow + 4NaCl + 5H_2O$

Calcination

For reducing impurity in prepared nano-materials, Calcination was done by placing them on Graphite crucible in furn at 700 C for 3 hours. After that, XRD, FTIR, and FESEM for CdO, MnO and the doping of CdO with MnO, then EDs tests were accomplished for each prepared nano-material except the doped nano- oxide.

RESULTS AND DISCUSSION

Phase Formation and Structural Analysis

The phase formation and structure analyses of synthesized nanoparticles before and after calcination are shown in Fig. 1, Fig. 2 and Fig. 3 along with the standard data for Cd_xO, Mn_xO and $Cd_xMn_{1-x}O$ nanoparticles respectively where [x= 0, 0.5 and 1].

The X-ray diffraction analyses were obtained from the Al-Khora Lab. In baghdad, Iraq using the XRD device manufactured in Malvern Panalytical, Company Head-quarters, Netherlands.

All the distinctive peaks of CdO were observed at 33.05°, 38.35°, 55.36°, 66.01°, 69.35° and 82.13° which were indexed to can be easily indexed to (111), (020), (022), (131), (222) and (040), crystal planes respectively before and after calcination; which are comparable with the standard values and suggested by literature [11]. While for MnO, all the distinctive peaks were observed at 23.10°, 32.91°, 38.19°, 45.11°, 49.28°, 55.12° and 65.68°,which were indexed to can be easily indexed to (121), (222), (040), (233), (134), (404) and (226) crystal

planes respectively before and after calcination; which are comparable with the standard values and suggested by literature [12]. All the distinctive peaks for doping of MnO with CdO were observed at 28.14°, 30.47°, 30.99°, 35.55°, 45.55°, 56.33 and 65.18°, which were indexed to can be easily indexed to (111), (310), (-311), (220), (112), (421) and (-223) crystal planes respectively before and after calcination; which are comparable with the standard values and suggested by literature [13].

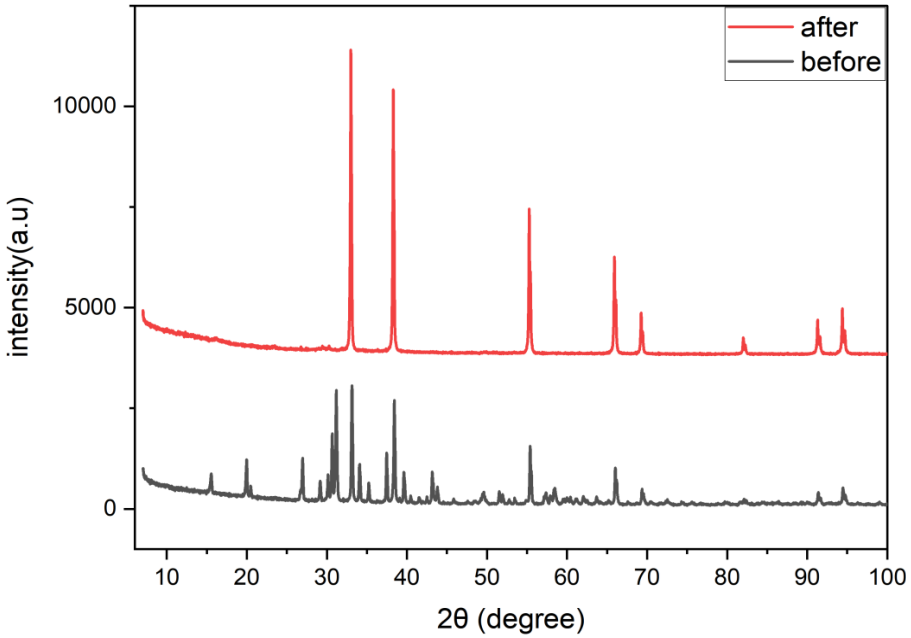

Fig. 2. XRD patterns of CdO before and after calcination.

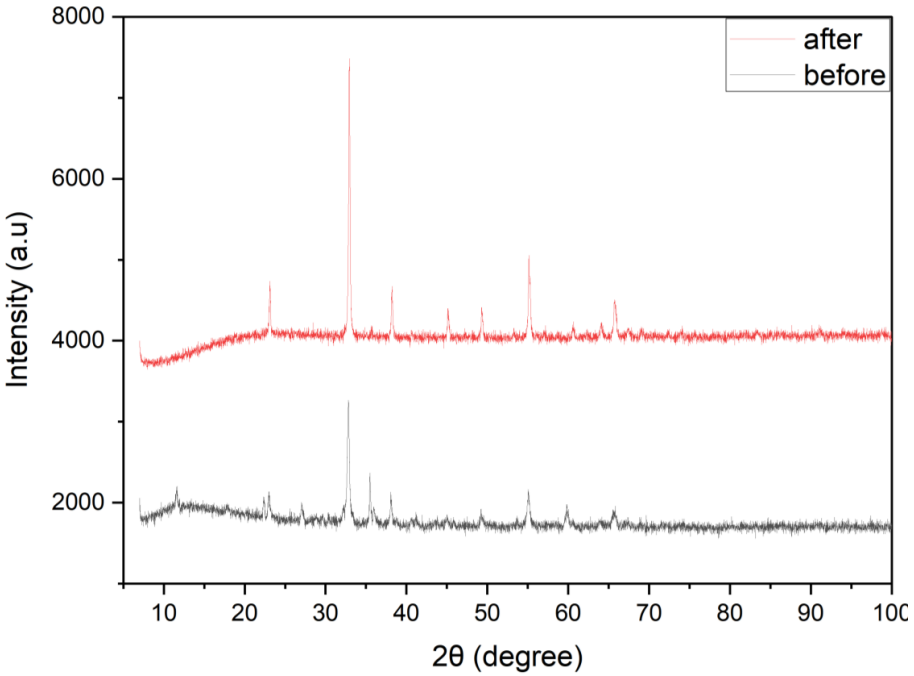

Fig. 3. XRD patterns of MnO before and after calcination.

The XRD patterns for the nano CdO, MnO and the doping of MnO with CdO revealed sharp diffraction peaks, confirming the formation of single-phase cubic structures for each oxide as shown in Fig. 2, Fig. 3 and Fig. 4 respectively before calcination. Calcination at 700 °C significantly reduced any residual hydroxide phases and improved crystallinity, as evidenced by the enhanced peak intensities [14]. Calcination lead to decreasing of the impurities and give good purity in the nano oxides [15] and that appeared in Fig. 2, Fig. 3 and Fig. 4 alternatively after calcination (shown by smoothing XRD curves).

Using Debye-Scherrer's equation [16] an average crystallite sizes (D) were calculated and described in the Table 1, D was ranged from 8.56 nm to 70.7 nm depending on the specific metal oxide. Lattice constants (a) of the corresponding nano materials were also obtained [17]. and summarized in Table 1.

The results in Table 1 shows increase in crystallize size of MnO with and without doping with CdO, while CdO show little decrease after calcination. Inversely to crystallize size, lattice constant show decreasing of MnO with and without doping with CdO, while CdO show increase after calcination. This result has no acceptance with (Hassan A., et,al.). revealed if the annealing temperature increases, the crystallite size increases gradually for CdO sample calcined at 700 °C, and the crystallite size direct has proportional with lattice constant [15].

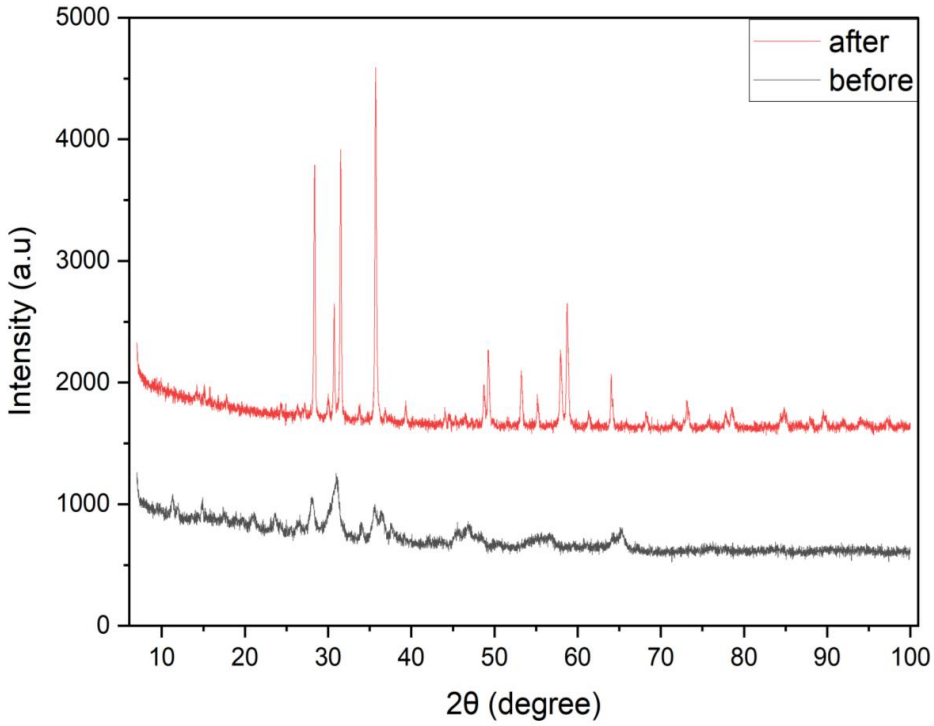

Fig. 4. XRD patterns of ($Mn_xCd_{1-x}O$) before and after calcination.

Table 1. Crystallite size and other Structure parameters of the Cd_xO, Mn_xO and ($Mn_xCd_{1-x}O$) nanopowders (where x = 0, 0.5, and 1) before and after calcination.

No.	Samples	2θ° (deg)	FWHM (deg)	d (A°)	D (nm)	a (A°)
1	CdO (before)	33.1097	0.1396	2.70344	61.96	4.6824
2	CdO (after)	32.976	0.1481	2.71409	58.47	4.7009
3	MnO (before)	32.7824	0.2593	2.72968	30.4	9.4558
4	MnO (after)	32.9078	0.1621	2.71956	62.2	9.4208
5	MnO+CdO (before)	30.8522	1.0058	2.8959	8.56	9.6046
6	MnO+CdO (after)	35.709	0.1519	2.5123	70.7	8.3323

FTIR Spectroscopy

FTIR spectra for Cd_xO, Mn_xO and $Mn_xCd_{1x}O$ nanopowders (where x = 0, 0.5, and 1) were recorded by Infrared Spectroscopy (Manufacturing by Shimadzu, Japan).

Before calcination there was strong absorptions in (400–600) cm^{-1} (Fig. 5) attributed to Cd–O stretching vibrations and its typical for CdO nanoparticles, low transmittance reflects the presence of surface-bound species and incomplete crystallinity. [18]. The absorptions in (500–650) cm^{-1} (Fig. 6) Mn–O stretching vibrations, confirming formation of MnO [19]. Broad peaks

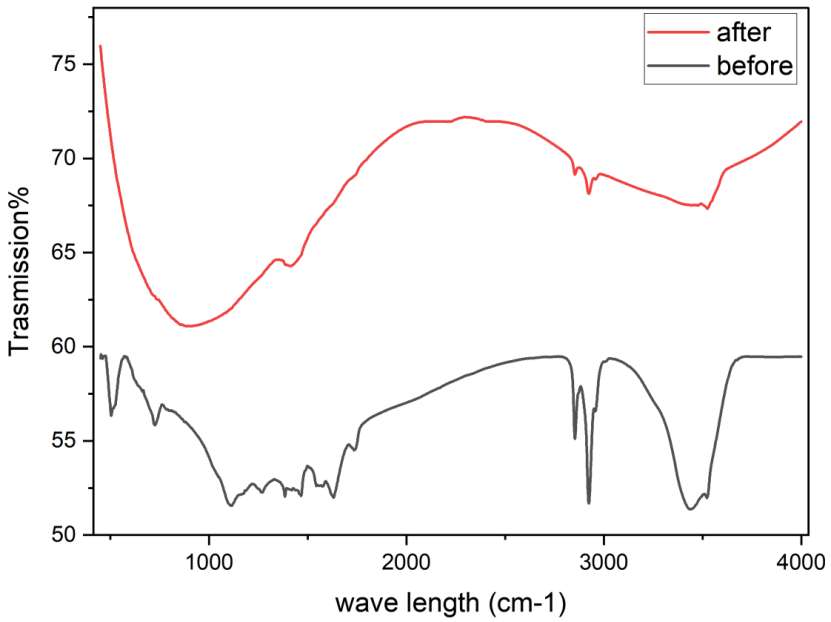

Fig. 5. FTIR spectrum for CdO before and after calcination.

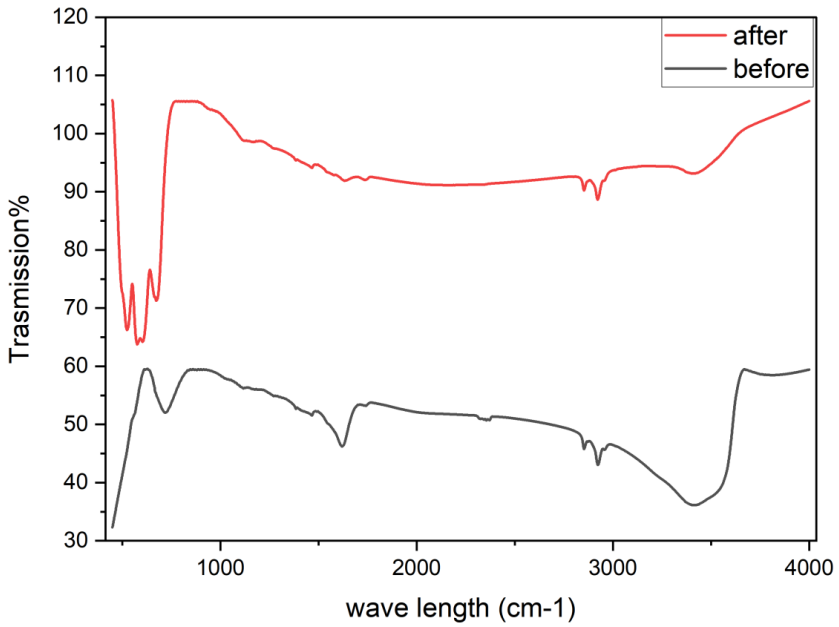

Fig. 6. FTIR spectrum for MnO before and after calcination.

showed in the (500–700) cm^{-1} range (Fig. 7) refer to overlap Cd–O and Mn–O stretching vibrations [20].

Also, before calcination showed characteristic metal–oxygen stretching vibrations were attributed to the stretching and bending modes of adsorbed water molecules shown in Fig. 5, Fig. 6 and Fig. 7 respectively.

After calcination, the reduction in these water-related peaks indicated successful removal of residual hydroxides and moisture [16], that seen clearly in Fig. 5, Fig. 6 and Fig. 7 alternatively.

Morphological analysis

The surface morphology for Cd_xO, Mn_xO and $Mn_xCd_{1-x}O$ nano powders (where x = 0, 0.5, and 1) were examined by direct observation using FE-SEM device kind [The Inspect F50 is manufactured by FEI, Thermo Fisher Scientific Inc.,Netherlands]. The FE-SEM images of all samples are depicted in Fig. 8, Fig. 9 and Fig. 10.

The FE-SEM images show the formation of CdO,

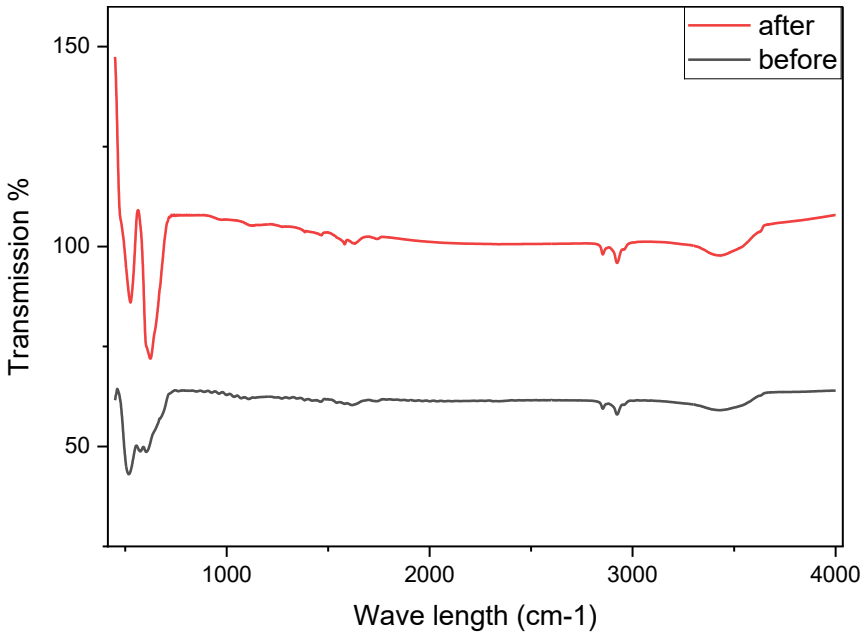

Fig. 7. FTIR spectrum for $Mn_xCd_{1-x}O$ before and after calcination.

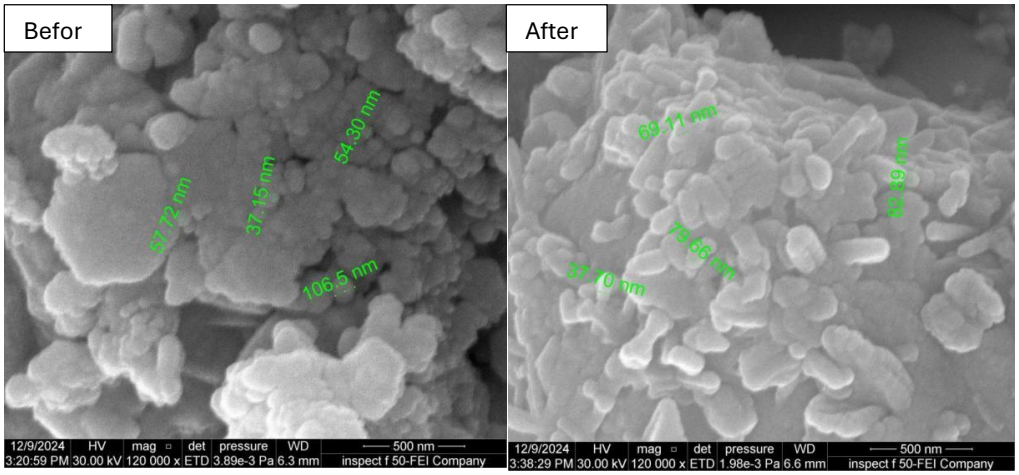

Fig. 8. FESEM for CdO before and after calcination.

MnO, and ($Mn_xCd_{1-x}O$) nanopowders (where x = 0, 0.5, and 1) possessed near-spherical or slightly agglomerated morphologies. The agglomeration ensues in nanoparticles owing to its magnetic nature and the binding of primary particles seized together by frail surface interaction such as Vander Waals force [21].

Also the voids and apertures in the images may be ascribed to the discharge of enormous volume of gas created by the decomposition throughout the combustion. Similar observed were seen in other ferrites [22]. The particle size distribution was relatively uniform, consistent with the XRD-based crystallite size estimates before calcination. The calcination process lead to increase agglomeration; that have no acceptance with another researcher that found the calcination helped to control particle growth and minimize agglomeration [17].

There was an elevation in the average particle size of samples that shown clearly in the FESEM test after calcination. The removal of residual organics and structural reorganization during calcination further contributes to agglomeration

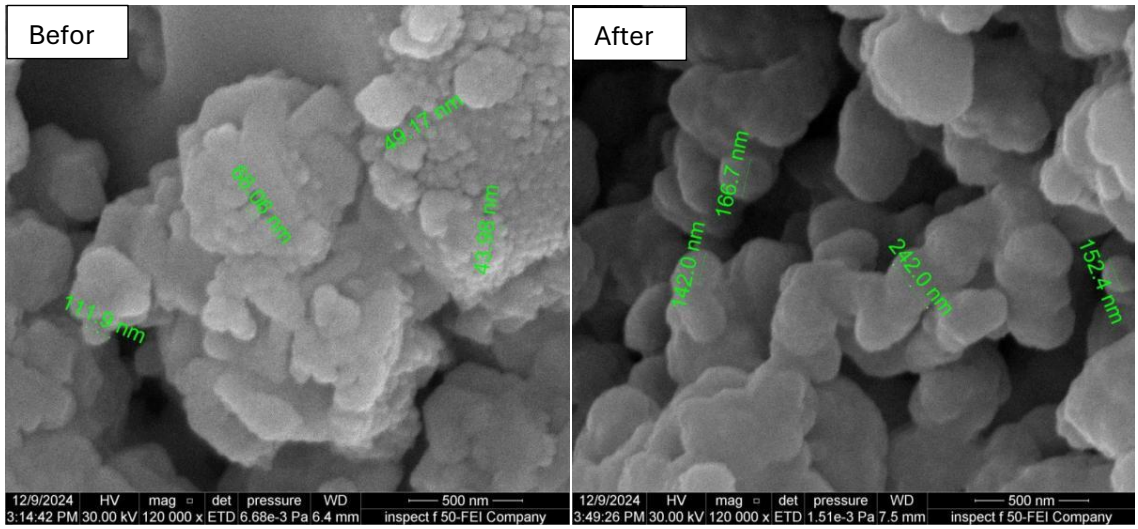

Fig. 9. FESEM for MnO before and after calcination.

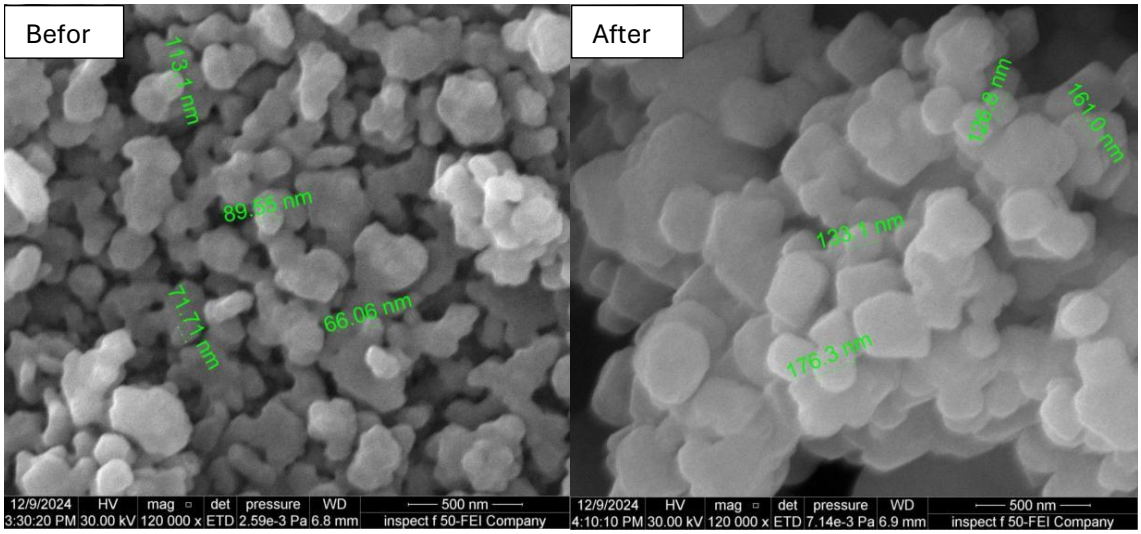

Fig. 10. FESEM for $Mn_xCd_{1-x}O$ before and after calcination.

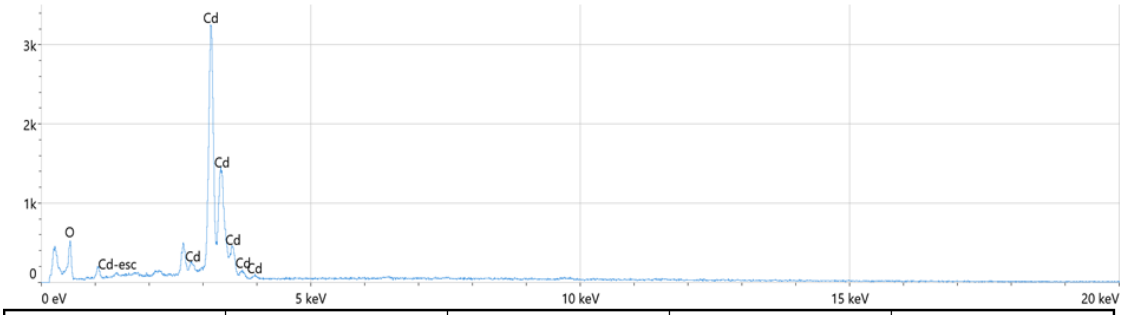

Element	Atomic %	Atomic % Error	Weight %	Weight % Error
O	74.4	1.9	29.3	0.8
Cd	25.6	0.3	70.7	0.7

Fig. 11. EDs for CdO after calcination.

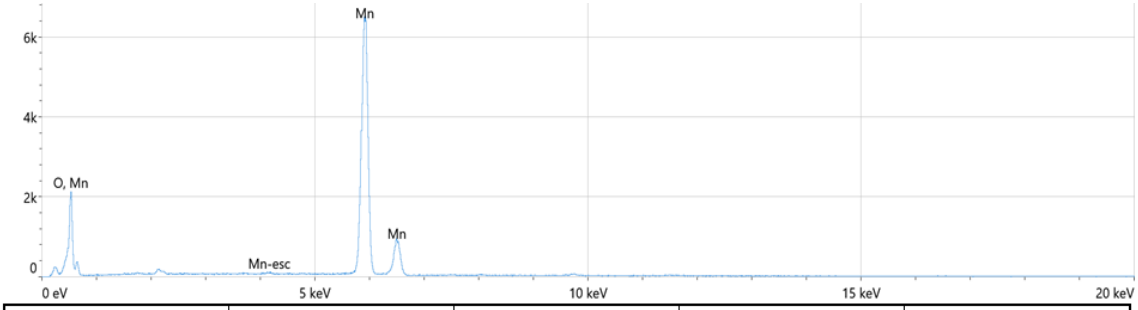

Element	Atomic %	Atomic % Error	Weight %	Weight % Error
O	44.7	0.6	19.1	0.2
Mn	55.3	0.3	80.9	0.4

Fig. 12. EDs for MnO after calcination.

and particle enlargement. Similar findings were reported for CdO and MnO systems, where higher calcination temperatures resulted in increased crystallite and particle sizes [23,24].

Energy dipersive X-ray spectroscopy (EDS)

EDS test is an analytical technique that enables the chemical characterization elemental analysis of materials [25,26]. The purity of nano oxides (Cd_xO and Mn_xO) after calcination (where x = 0, 0.5, and 1) were accomplished by EDs test that show the peaks and percent of the elements Fig. 11 and Fig. 12.

CONCLUSION

CdO and MnO NPs provide a wide range of possible uses due to their unique properties. Detailed structural and morphological investigations using XRD revealed the change in the lattice constants and particle sizes of the CdO and MnO. Crystalline size and lattice constant have inverse relationship before and after calcination where increasing in crystallize size lead to decrease in the lattice constant and vice versa. Also, calcination affects lead to improve crystallinity and decreasing of the impurities and give good purity in the nano oxides, increase particle size and altering morphology, reduction in these water-related peaks that indicated successful removal

of residual hydroxides and moisture. This leads to enhanced transmission and sharper metal–oxygen bands in FTIR, and finally increase agglomeration.

CONFLICT OF INTEREST

The authors declare that there is no conflict of interests regarding the publication of this manuscript.

REFERENCES

1. Yang J, Fan L, Xu Y, Xia J. Iron oxide nanoparticles with different polymer coatings for photothermal therapy. J Nanopart Res. 2017;19(10).
2. Preston GD. Elements of X-ray Diffraction by B. D. Cullity. Acta Crystallogr. 1957;10(5):389-389.
3. Long DA. Infrared and Raman characteristic group frequencies. Tables and charts George Socrates John Wiley and Sons, Ltd, Chichester, Third Edition, 2001. Price £135. J Raman Spectrosc. 2004;35(10):905-905.
4. Tilley RJD. Defects in Solids: Wiley; 2008 2008/02/29.
5. Nanoparticles and Catalysis: Wiley; 2007.
6. Wang C, Yin L, Zhang L, Xiang D, Gao R. Metal Oxide Gas Sensors: Sensitivity and Influencing Factors. Sensors. 2010;10(3):2088-2106.
7. Anuradha CT, Raji P. Synthesis, Characterization and Anti-Microbial Activity of Oxalate-Assisted CO_3O_4 Nanoparticles Derived from Homogeneous Co-Precipitation Method. International Journal of Nanoscience. 2019;18(05):1950002.
8. Sun L. One-dimensional nanostructured materials for energy storage applications: Nanyang Technological University.
9. M V, P RP, R A, K S, Suresh S, S G, et al. Comparison of sunlight-driven photocatalytic activity of semiconductor metal oxides of tin oxide and cadmium oxide nanoparticles. Optik. 2020;217:164878.
10. Vijayaprasath G, Murugan R, Asaithambi S, Sakthivel P, Mahalingam T, Hayakawa Y, et al. Structural and magnetic behavior of Ni/Mn co-doped ZnO nanoparticles prepared by co-precipitation method. Ceram Int. 2016;42(2):2836-2845.
11. Zhang J. Room-temperature compressibilities of MnO and CdO: further examination of the role of cation type in bulk modulus systematics. Phys Chem Miner. 1999;26(8):644-648.
12. Rebane E. Mass Spectra of Some Aliphatic and Aromatic Selenides. Acta Chem Scand. 1973;27:2861-2869.
13. Oswald HR, Wampetich MJ. Die Kristallstrukturen von Mn5O8 und $Cd_2Mn_3O_8$. Helv Chim Acta. 1967;50(7):2023-2034.
14. Biju V. Chemical modifications and bioconjugate reactions of nanomaterials for sensing, imaging, drug delivery and therapy. Chem Soc Rev. 2014;43(3):744-764.
15. Muhammad W, Muhammad Niamat Ullah B, Saima M, Shehla M, Bushra Z, Ruqia N, et al. Impact Assessment of Import Substitution and Export Promotion on Economic Growth of Pakistan. Journal for Social Science Archives. 2025;3(2):685-691.
16. Akbar H, Javed MS, Parveen B, Ahmad A, Ali A, Abukhadra MR, et al. Investigating the Effects of Calcination Temperature on CdO Nanorods for Performance of Advanced Supercapacitors. J Electrochem Soc. 2025;172(3):033501.
17. Huang X, Jain PK, El-Sayed IH, El-Sayed MA. Plasmonic photothermal therapy (PPTT) using gold nanoparticles. Lasers Med Sci. 2007;23(3):217-228.
18. Gawande MB, Goswami A, Asefa T, Guo H, Biradar AV, Peng D-L, et al. Core–shell nanoparticles: synthesis and applications in catalysis and electrocatalysis. Chem Soc Rev. 2015;44(21):7540-7590.
19. Bindhu MR, Umadevi M, Kavin Micheal M, Arasu MV, Abdullah Al-Dhabi N. Structural, morphological and optical properties of MgO nanoparticles for antibacterial applications. Mater Lett. 2016;166:19-22.
20. Yang G, Li Y, Ji H, Wang H, Gao P, Wang L, et al. Influence of Mn content on the morphology and improved electrochemical properties of Mn_3O_4|MnO@carbon nanofiber as anode material for lithium batteries. J Power Sources. 2012;216:353-362.
21. Manjula N, Pugalenthi M, Nagarethinam VS, Usharani K, Balu AR. Effect of doping concentration on the structural, morphological, optical and electrical properties of Mn-doped CdO thin films. Materials Science-Poland. 2015;33(4):774-781.
22. Kombaiah K, Vijaya JJ, Kennedy LJ, Bououdina M. Optical, magnetic and structural properties of $ZnFe_2O_4$ nanoparticles synthesized by conventional and microwave assisted combustion method: A comparative investigation. Optik. 2017;129:57-68.
23. Navale ST, Bandgar DK, Nalage SR, Khuspe GD, Chougule MA, Kolekar YD, et al. Synthesis of Fe 2 O 3 nanoparticles for nitrogen dioxide gas sensing applications. Ceram Int. 2013;39(6):6453-6460.
24. Li B, Ji Z, Xie S, Wang J, Zhou J, Zhu L. Electromagnetic wave absorption properties of carbon black/cement-based composites filled with porous glass pellets. Journal of Materials Science: Materials in Electronics. 2019;30(13):12416-12425.
25. Vanhellemont J, Simoen E. On the diffusion and activation of n-type dopants in Ge [Mater. Sci. Semicond. Process. 15 (2012) 642–655]. Mater Sci Semicond Process. 2014;17:184-185.
26. Newbury DE, Ritchie NWM. Performing elemental microanalysis with high accuracy and high precision by scanning electron microscopy/silicon drift detector energy-dispersive X-ray spectrometry (SEM/SDD-EDS). Journal of Materials Science. 2014;50(2):493-518.